ISSN 1330–0016
CODEN FIZBE7

# A NOVEL SYSTEM FOR PARTICLE IDENTIFICATION IN THE 3.0–8 GeV/$c$ RANGE

SINICHI ESUMI[a], CHRISTIAN W. FABJAN[b], ACHIM FRANZ[b], BARBERA HOLZER[b,f], MASASHI KANETA[a], GUY PAIĆ[c,g], FRANCOIS PIUZ[b], JEAN-CLAUDE SANTIARD[b], JANUS SCHMIDT-SORENSEN[d], MARKO SPEGEL[b], TORN SUGITATE[a] and THOMAS D. WILLIAMS[b]

[a] *Hiroshima University, Higashi, Hiroshima, Japan*
[b] *CERN, Geneva, Switzerland*
[c] *Subatech, Nantes, France*
[d] *Niels Bohr Institute, Copenhagen, Denmark*
[f] *Technical University, Vienna, Austria*
[g] *On leave of absence from Rugjer Bošković Institute, Zagreb, Croatia*

**Dedicated to Professor Mladen Paić on the occasion of his 90$^{\text{th}}$ birthday**

Received 13 July 1995

UDC 539.1.074

PACS 29.40.Ka

A threshold imaging Cherenkov (TIC) detector, in conjunction with a tracking device, has been developed to allow pion/kaon, proton identification in the 3–8 GeV/$c$ range of momenta. The most important feature of the system is that it allows spatial identification of the photons of particles above the Cherenkov threshold and their correlation to a particular track. The TIC detector uses a MWPC detector with TMAE for photon conversion into electrons. The first results obtained in ultrarelativistic lead–lead collisions at the CERN SPS accelerator are presented. In a recent development use of a solid CsI cathode instead of TMAE has been successfully tested in proton–lead collisions at the CERN SPS.

## 1. Introduction

In high-energy physics experiments one is often confronted with the need to identify particles in a wide momentum range — from several hundreds to several thousands of MeV/$c$. Especially arduous is the task of identifying particles in the 3.5–7 GeV/$c$ range. In this range many conventional approaches (d$E$/d$x$, liquid radiator RICH detectors, TOF detectors) have considerable difficulties in achieving simultaneous identification of pions, kaons and protons. The use of Cherenkov threshold detectors for identification is possible in cases where the density of particles is low, but is not practical in applications where a high density of particles is expected, as is the case in ultrarelativistic nucleus–nucleus collisions. To circumvent this, and still benefit from the properties of threshold Cherenkov detectors, we have built a system for imaging the photons produced by particles above threshold (i.e. the position of each individual photon is recorded in the detector plane), by which full information on the position of the emitted photons can be kept. Using this device, it is possible to achieve a very high granularity for a limited cost using pad-segmented MWPC's for UV photon detection, therefore allowing complex pattern recognition otherwise difficult to achieve with conventional threshold detectors. By combining the threshold imaging Cherenkov (TIC) detector with a time-of-flight wall (TOF), complete identification of pions, kaons and protons in the 3.0–8 GeV/$c$ range is possible. The detector system has been conceived for the heavy-ion experiment NA44, currently running at the CERN SPS. We present a description of the new detector, as well as a preliminary analysis of the data taken in collisions of lead ions on a lead target in November 1994 at the CERN SPS. In the detector used last year, the photoionization was achieved using TMAE vapour. However, the recent encouraging results of the CERN RD26 [1] collaboration on the development of solid CsI photocathodes has prompted a test of the TIC with a CsI photocathode in 200 GeV/$c$ lead proton collisions, and these results are also presented.

## 2. The NA44 experiment

NA44 [2], the "focusing spectrometer", is a second-generation relativistic heavy-ion experiment at the CERN SPS accelerator, designed for measuring two-particle correlations and single-particle spectra over a wide range of rapidity and transverse momenta. The spectrometer is equipped with trigger devices allowing triggering on single particles or pairs of rare particles. NA44 uses superconducting quadrupoles and warm-dipole magnets to produce a magnified image of the target on the tracking detectors–two hodoscopes, pad and strip chambers. The tracking information defines the momentum, whilst the timing information from the scintillation hodoscopes (time resolution–100 ps) defines the velocity and therefore the mass of the particles. The online particle identification is further aided by two gas threshold Cherenkov counters. However, the increased multiplicity of particles of Pb–Pb collisions at 160 A GeV/$c$ made it necessary to complement the setup with the TIC, allowing offline identification.

## 3. TIC operating principle and main components

The TIC detector principle of operation is based on the 2D-localization of the Cherenkov photons created in a gas volume, where pions are above the Cherenkov threshold and kaons and protons are below it. The spatial information, correlated with the tracking information, allows unequivocal identification of pions. The identification of kaons and protons is achieved using the TOF information.

The TIC detectors main components are: the radiator where the UV photons are created, with two 45° mirrors, the photon detector and the heat and gas container. In Fig. 1 we show a schematic view of the TIC detector.

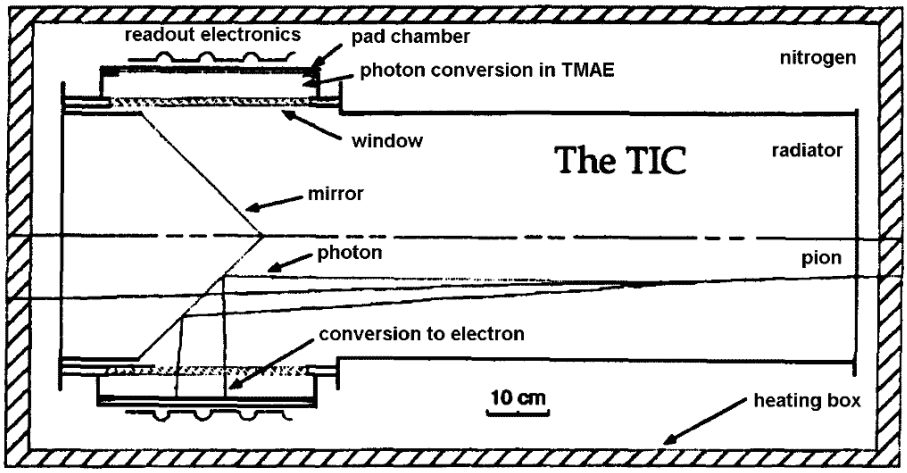


*Fig. 1. Schematic view of the threshold imaging Cherenkov (TIC) detector.*

Also, trajectories of two photons are represented that are created by a pion (in reality a pion will emit in the wavelength range of interest 50–100 photons, depending on its momentum). The photons are created along the pion path in the radiator under the characteristic Cherenkov angle given by

$$\cos\theta = \frac{1}{n\beta} \ ,$$

where $n$ is the refractive index and $\beta$ is $v/c$ of the particle. The photons are reflected by two mirrors placed at 45° to the radiator axis, and enter the photon detector through a UV-transparent quartz window. A particle of mass $m$, of momentum above the Cherenkov momentum threshold $p^t$ given by

$$p^t = m\left(\frac{1}{\sqrt{1-1/n^2}} - m\right) \ ,$$

will result in a number of photons being detected in the TIC within a fiducial disk, created by the projection of the cone of creation of photons in the radiator onto the detector plane. The purpose of the mirrors is the following: to avoid the superposition of the charged particles (by the ionization in the detection chamber) were the TIC chambers placed in the spectrometer acceptance. In the present setup ideally no signal is read in the TIC chamber for a particle below threshold.

The two-mirror solution was adopted to minimize the difference in the radiator length within the acceptance, and also for an easier construction of the photon detectors.

### *3.1. Radiator*

The radiator consists of a 130 cm×90 cm×40 cm tank, filled with isobutane at atmospheric pressure. The gas is continuously flushed through an Oxysorb purifier cartridge. The transparency of the gas is controlled by a UV monochromator.

Isobutane was chosen as a convenient radiator because of its refractive index ($n = 1.0017$ for photons of 7 eV), resulting in a threshold momentum of 2.2 GeV/$c$, and 7.9 GeV/$c$ for pions and kaons, respectively, which allows spanning of the whole range of interest. Another gas with a similar refractive index is $C_4F_{10}$, but its high price and the necessity of having a closed circulation made isobutane a simpler and more cost efficient solution. However, it should be mentioned that $C_4F_{10}$ has much better transparency in UV than isobutane, so that by using the former with a highly transmissive $CaF_2$ window, one could obtain results equivalent in quality to the ones presented here with a shorter radiator. The radiator length was fixed at 1 m, as an appropriate compromise between the number of photons finally detected and the spread of the photon fiducial disc in the detector (if the radiator length is too great, then attributing a specific photon disc to a specific track may be difficult in the case of close tracks). The possibility of using a gas with higher transparency may be important when dealing with higher multiplicities then we met. In our case the radius of the photon fiducial disk in the chamber is 5 cm.

### *3.2. Mirrors*

The mirrors were made of 2 mm glass with a UV reflective Al coating, covered with a thin layer of $MgF_2$. To prevent the mirrors sagging, a supporting frame was constructed, and the edges of mirrors edges were reinforced by a thin aluminium $L$ profile mounted to bind them at the central edge.

### *3.3. Photon detector and front-end electronics*

The photon detector is a classical multiwire proportional chamber (MWPC), preceded by a conversion gap. The principle of operation is shown schematically in Fig. 2. The photons created in the radiator enter through a 5 mm quartz window into a conversion gap in which they convert into electrons by photoionization of

tetrakis (dimethyl) aminoethylene (TMAE), which is added in the form of saturated vapour to the detector gas (methane). As TMAE is a liquid at normal temperatures, it is necessary to bubble the detector gas through liquid TMAE. The quantity of TMAE vapour in the gas is determined by the temperature of the bath in which the bubbling is done.

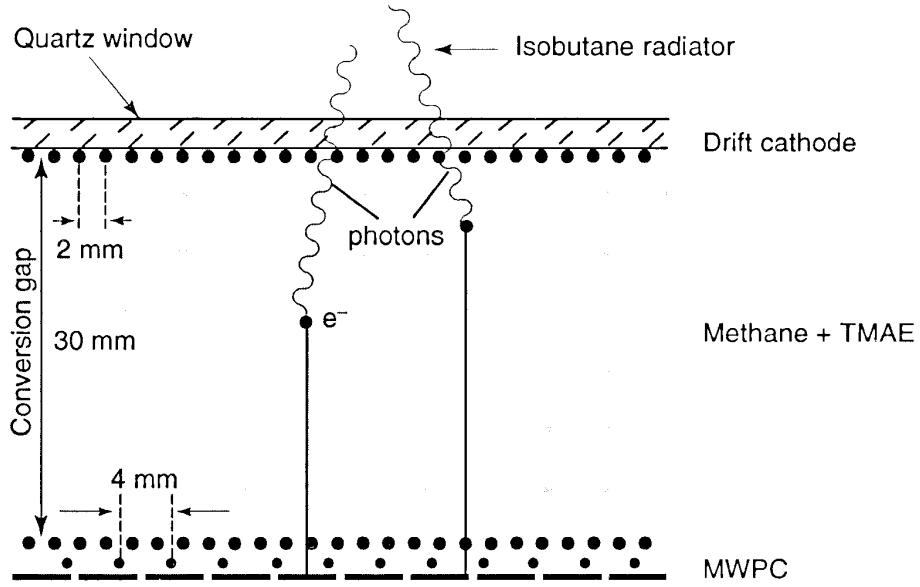


*Fig. 2. Main parts of the UV photon detection system.*

After photoionization in TMAE, the photoelectron drifts toward the MWPC in a field of about 400 V/cm. Once the electron is in the MWPC volume, multiplication occurs at the anode wire, causing an induced signal on the pads (8 mm × 8 mm) of the second cathode.

The length of the conversion gap is determined by the mean free path of UV photons in TMAE vapour. The dependence of the mean free path of a photon in TMAE is given by the empirical formula

$$L_0(T) = 6.3/(\mathrm{e}^{-T/18}) \ ,$$

where $L_0$ is in centimetres and $T$ in centigrade. Under our conditions, the temperature of the bubbler was 25 °C and the gap length 30 mm, ensuring full absorbtion of the incoming photons. The technical specifications of the TIC photon detectors are given in Table 1.

*TABLE 1.*
*Technical specifications for the TIC photon detection chambers.*

| | |
|---|---|
| active area | 78 cm × 19 cm |
| number of pads | 96 × 24 |
| pad size | 8 mm × 8 mm |
| pad-plane composition | 35 $\mu$m Cu + Au on 1 mm G10 |
| chamber gas | $CH_4$ + TMAE |
| quartz-window thickness | 5 mm |
| half-gap | 2 mm |
| conversion gap | 30 mm |
| anode-wire pitch | 4 mm |
| anode-wire diameter | 20 $\mu$m |
| cathode-wire pitch | 2 mm |
| cathode-wire diameter | 100 $\mu$m |

The signal, induced by the charge amplification, is processed analogically by a 16-channel AMPLEX chip [3], originally designed for silicon detectors but very successfully used in MWPCs. The AMPLEX chip consists of a charge amplifier, shaping amplifier, track and hold, and multiplexing stage.

The important feature of the electronics is their long integration time 500 ns. This allows a large induced signal, keeping the amplification in the MWPC at a relatively low level of $10^5$, even for single electrons, as is the case in the detection of Cherenkov radiation [4]. The integration time is still sufficiently small to allow applicability in all cases where the detection rate is below $10^5$ Hz.

The readout of the AMPLEX chips is made by the digital readout system for analog multiplexing signals (DRAMS) [5]. In the DRAMS modules, the signals are digitized using an 8-bit flash ADC, and compared to a pedestal/threshold memory. At the beginning of each run, a pedestal run is taken (without beam). From this run, two parameters are determined for each channel: the value of the pedestal, and the width of the pedestal distribution. The digitized amplitudes are compared to a threshold map before recording and the threshold value is taken to be the mean of the pedestal distribution for each channel:

$$\text{threshold} = \text{pedestal} + N \times \sigma \ .$$

Only the values exceeding the threshold are recorded.

In Fig. 3 we show the single electron pulseheight distribution obtained with the TIC using $N = 3$ for the threshold. The spectrum is exponential–a feature typical of single electron amplification in gases. The values of $N = 3 - 4$ are used in the analysis and result in a single electron detection efficiency of 80 – 90%.

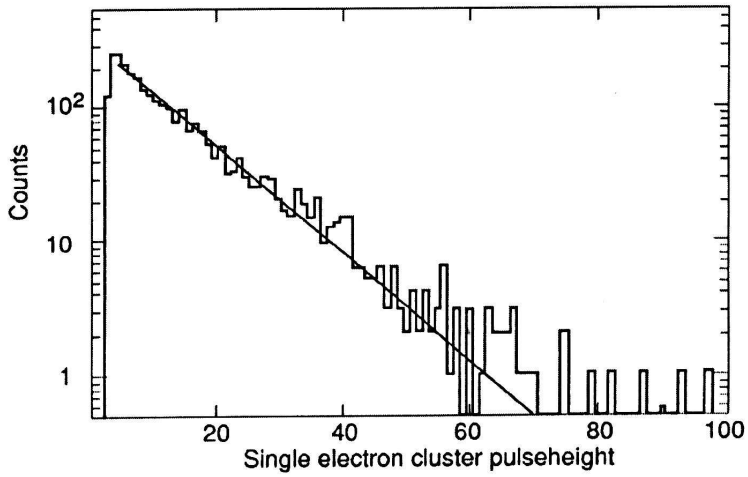


*Fig. 3. Single photoelectron spectrum measured on the cathode pads, exhibiting the characteristic exponential shape.*

### *3.4. Heating and insulation*

The radiator and detector assembly are placed in a gastight container flushed with nitrogen, as isobutane and air would produce an explosive mixture if there were a leak in the radiator. Water circulates through the walls of the container to heat the detector gas above the temperature of the bubbler bath (30 °C in our case).

## *4. Results of measurements of Pb–Pb collisions*

The two TIC photon detection chambers were tested in the first lead-ion beam run at the SPS in November 1994, in conjunction with the particle spectrometer of the NA44 collaboration.

In Fig. 4 we show several events observed in the Pb–Pb runs. The circles define the fiducial area around the track impact point (star), mirror reflected on the TIC plane. Both photon detection chambers are combined in a single plane in the figures. Event 50 shows two pions in the acceptance and a number of pads hit in the upper right part of the TIC. Judging by the amplitude (higher than the single photoelectron signal), and the topology (not disc-like), we conclude that this is most probably caused by a charged particle passing through the active volume of the photon detector (conversion gap and MWPC width).

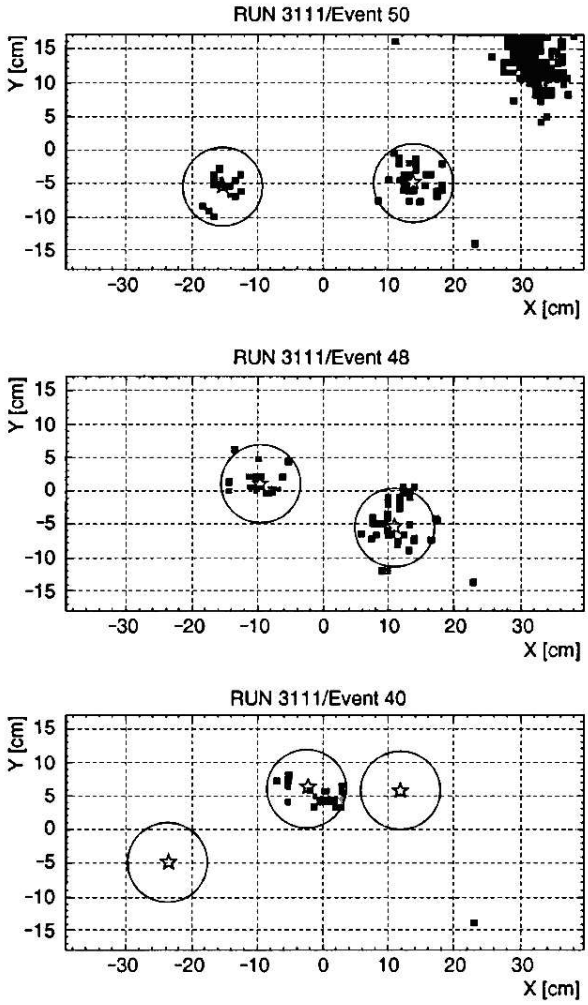


*Fig. 4. Typical events recorded in* Pb–Pb *collisions. The stars mark the particle track impact brought to the TIC plane; the shades of grey show the intensity of the charge induced on individual pads.*

The TIC chambers are outside the acceptance of the spectrometer, but are irradiated by neutrons from the lead beam dump. Indeed, we have observed an important increase in the detector current during the beam spill. During the spill ($4 \times 10^6$ particles on target) the current would increase to 400–500 nA, compared to just a few nanoamperes without beam, limiting our ability to make the optimum choice of high voltage bias. Other sources of background have also been identified, namely cases when a secondary particle produced in the spectrometer, but not identified as a valid track by the tracking algorithm, creates a photon disc in the

TIC. The other two events displayed in Fig. 4 show examples of a two-pion event without any background, and a case when there were three tracks in the acceptance, but only one belonging to a pion (further identification to distinguish whether it is a pion or a kaon is done using the TOF information).

In Fig. 5 we show a two-dimensional plot of the TIC, analysed in conjunction with the TOF wall. For each track, the mass-square value is given by

$$m^2 = p^2(T^2/L^2 - 1) \ ,$$

where $p$, $T$ and $L$ are the momentum, the time-of-flight and the path length, respectively. The results are displayed in two dimensional plot figuring the number of pads detected in the fiducial area of the TIC versus the square of the mass obtained from the TOF information corresponding to the same track. From the plot, one can see that the purpose of the system has been achieved–positive identification of pions by hits in the TIC, and identification of the kaons and protons by the absence of hits in the TIC and the making of the appropriate cuts on the mass-square axis. From Fig. 5 we see clearly the islands corresponding to pions, kaons and protons. The purpose of the TIC is also demonstrated since if only the $M^2$ information would be used a contamination of kaons by pions would ensue. Also from Fig. 5 it is clear that for a small fraction of events, the kaons and protons have hits in the TIC. We attribute these to accidental overlap of hits belonging to the background sources within the fiducial areas. A mean number of 19 pads were hit in each fiducial area. The distribution is larger than Gaussian due to slight differences in the MWPC gain across the TIC chamber. Nevertheless, it is apparent that very good pion/kaon separation was achieved because, although pions do contaminate the kaons in the mass square spectrum alone, the number of pads hit in the TIC clearly indicates that the particle not identified in the TOF spectrum is a pion.

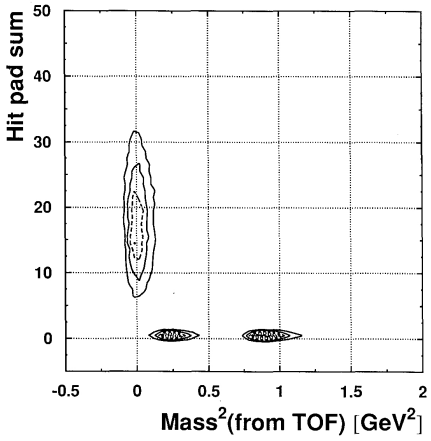


*Fig. 5. A two dimensional view of the TIC results. The number of pads hit in one plane are brought on one axis, whilst on the other axis is the M-squared value obtained from time-of-flight measurements.*

It is important to mention that these data were taken at the 4 GeV/$c$ setting of the spectrometer (the measuring range of NA44 is 4–8 GeV/$c$), where the TOF is still relatively good and the number of photons from the radiator is at its lowest in the whole range of exploitation. Furthermore, a more sophisticated analysis of the data could recognize and discriminate to a large extent the background hits due to either a different topology or pulseheight or both.

## 5. *CsI photocathode*

As mentioned above, during the Pb-beam runs, we encountered problems linked to the background radiation present in our environment. Besides taking measures to reduce that background by additional shielding, there is also the possibility of reducing the sensitivity of the detector to charged particles. This is most efficiently done by reducing the sensitive volume of the detector–in our case by reducing the conversion gap. This conversion gap reduction means either considerably increasing the temperature of the TMAE bath, which introduces considerable stress on the structure of the whole detector, or using a solid photocathode evaporated on the pad-cathode plane. With the conversion occurring on a thin (500 nm) layer, the active depth of the detector for collection of electrons is reduced to the thickness of the MWPC proper, 4 mm, instead of the previous depth of 34 mm.

Since 1992, the RD26 collaboration [6] has actively pursued the development of large-area solid photocathodes operating in a MWPC. The cathode consists of a thin film of CsI evaporated on the pad-cathode plane. Recently, technology has been developed for producing the substrates for the photocathode in such a way that the CsI quantum efficiency for photoionization is kept at the level of small samples with specially treated surfaces [1].

### 5.1. *Photocathode production*

The photocathodes have been prepared using the following procedure: a circuit board consisting of a copper layer on a G10 foil was used to produce the pad pattern, involving standard etching techniques; the pad–printed board was then polished using alumina paste and chemical polishing, and a thick homogeneous layer of nickel (15 $\mu$m) was chemically deposited, followed by a gold layer on top of the nickel one. Onto these substrates, CsI was evaporated under high vaccuum to form a 500 nm layer. After evaporation, the photocathode was heat-treated for five hours at a temperature of 50 °C. Such photocathodes have been found to have a surface structure and quantum efficiency equivalent to those observed in small polished metallic surfaces.

The photocathode used in the present test is, to our knowledge, the largest CsI photocahthode so far tested.

### *5.2. Test results*

The test was conducted with 200 GeV/$c$ protons at the CERN SPS, using only one of the two TIC chambers described. The NA44 spectrometer was set to the 4 GeV/$c$ setting, as in the case of Pb–Pb, described earlier. In order to be able to keep the existing chamber design with the large conversion gap, we neutralized it by applying a reverse drift field that collects all the electrons produced in the gap on the electrode near the quartz window shown in Fig. 2. In Fig. 6 we show an overlap of many events obtained with the solid-state photocathode. The overlap illustrates the full disc-size of the photons in the TIC plane, the size of the dark spots representing the number of detected photons. The falling intensity towards the edges has two causes–the outermost photons come from the upstream part of the radiator and are hence more absorbed, and on the other hand, the visual effect is in need of correction for the larger size of the outer ring. Preliminary analysis has shown the overall behaviour of the TIC with a solid photocathode comparing favorably with the performance when TMAE is used. The related performance provides significant ease of operation, eliminating the need for heating the detector system. The suppression of the conversion gap allows the running of the detector in a high-radiation environment.

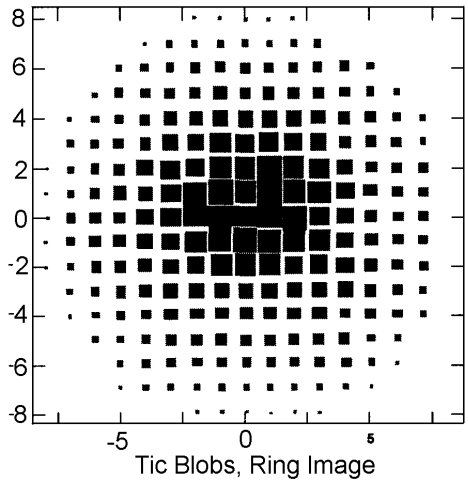


*Fig. 6. The photon disc in the TIC obtained by superimposing many events.*

## *6. Conclusion*

A device, combining the easy particle identification of a threshold Cherenkov counter and the possibility of identifying the Cherenkov signal track-by-track, has been achieved using an isobutane radiator and MWPC equipped with a photon conversion gap. The photon conversion was done using TMAE gas in the detector used for physics runs in the NA44 spectrometer in November 1995. Recently, a

test run was successfully performed using a solid CsI photocathode for the photon conversion. The photocathode produced is the largest one used so far in a test. Preliminary results have shown very satisfactory results.

Coupled to a TOF system, the TIC can successfully identify pions, kaons and protons in the 3–8 GeV/$c$ range.

Acknowledgements

One of us (G.P.) wishes to express his gratitude to Drs. M. and V. Paić for his initiation into experimental physics, love, encouragement and constant interest.

References

1) J. Almeida, A. Amadon, P. Besson, P. Bourgeois, A. Braem, A. Breskin, A. Buzulutskov, R. Chechik, C. Coluzza, A. Di Mauro, J. Friese, J. Homolka, A. Ljubicić jun., G. Margaritondo, Ph. Miné, E. Nappi, T. dell'Orto, G. Paić, F. Piuz, F. Posa, J.C. Santiard, S. Sgobba, G. Vasileiadis and T. D. Williams, *Review of the development of large Cesium iodide Photocathodes for application to large RICH detectors*, presented at the Wire Chamber Conference, Vienna, Feb. 1995, to be published in Nucl. Instrum. Meth. Phys. Res. and CERN–PPE/95–63;

2) H. Boggild et al., Phys. Lett. **B302** (1993) 510;

3) E. Beuville, K. Borer, E. Chesi, E. Heijne, P. Jarron, B. Lisowski and S. Singh, Nucl. Instrum. Meth. Phys. Res. **A288** (1990) 157;

4) A. Braem, A. Di Manzo, E. Nappi, A. Ljubičić Jr., G. Paić, F. Piuz, F. Posa, R. S. Ribeiro, T. Scognetti and T. D. Williams, Nucl. Instrum. Meth. Phys. Res. **A343** (1994) 163;

5) E. Chesi et al., *Digital Readout for Analog Multiplexed Signals*, PS Note 202, CERN 1988;

6) F. Piuz, A. Braem, G. Paić, R. S. Ribeiro and T. D. Williams, Nucl. Instrum. Meth. Phys. Res. **A333** (1993) 404. Berlin, 1966.

## NOV SISTEM ZA IDENTIFIKACIJU ČESTICA U PODRUČJU $3 - 8$ GeV/c

Razvijen je pozicioni detektor fotona Čerenkovljeva zračenja iznad praga emisije (TIC), koji omogućuje (u sklopu sistema za mjerenje tragova čestica) razlikovanje piona od kaona i protona u podrucju između praga emisije za pione i za kaone t.j između 3 i 8 GeV/c. Najbitnija odlika sistema jest mogućnost dvodimenzijske lokalizacije emitiranih fotona i njihovo jednoznačno pridruživanje određenom tragu čestice koji je određen drugim detektorima. Detektor TIC primjenjuje višezičane proporcionalne komore s TMAE dodanom brojačkom plinu za konverziju fotona u elektrone. Prikazuju se prvi rezultati dobiveni u ultrarelativističkim sudarima iona olova s metom olova u SPS akceleratoru u CERNu. Nedavno je upotreba čvrstih fotokatoda umjesto TMAE bila uspješno iskušana procesima sudara protona s olovom u SPS akceleratoru.